The 4-Day Wave and Transport of UARS Tracers in the Austral Polar Vortex

G. L. Manney,
Jet Propulsion Laboratory/California Institute of Technology, Pasadena, USA

Y. J. Orsolini,
Centre National de Recherches Météorologiques, Toulouse, France

H. C. Pumphrey,
Department of Meteorology, University of Edinburgh, Edinburgh, UK

A. E. Roche,
Lockheed Martin Palo Alto Research Laboratory, Palo Alto, USA

Received ______________________; accepted ______________________

Submitted to *Journal of the Atmospheric Sciences,* August 1997

Abstract

UARS tracer data and isentropic transport calculations using UKMO winds initialized with these data show evidence of eastward-traveling waves in the polar upper stratosphere in late austral winter 1992. MLS H_2O from prototype iterative retrievals shows a 4-day wave signal at levels from ~1 .5- 0.1 hPa; a 4-day wave signal was not obvious in production retrievals of MLS H_2O. At 1800 K, the 4-clay wave in MIS H_2O has a double-peaked structure in latitude, which is reproduced in isentropic transport calculations. The time evolution, amplitude and phase of the 4-day wave in the transport calculations agree well with observations at high-latitudes; the position and shape of the polar vortex and of H_20 drawn up around the vortex are reproduced by the transport calculations. Spectral analysis of CLAES CH_4 shows a 4-day wave signature between ~4 and 1,5 hPa, with slower eastward-moving wave features (periods near 6-10 days) below ~2 hPa. Transport calculations initialized with CH_4 show similar eastward-traveling signals, good agreement with the phase of the observed signals, and overall agreement with the observed position of the vortex. The success of the transport calculations in qualitatively reproducing the phase and time evolution of high-latitude eastward-traveling waves in the polar upper stratosphere indicates that the winds used for the transport calculations are generally reliable, and that the eastward-traveling waves identified in the MLS H_20 and CLAES CH_4 originate to a large extent from horizontal transport processes. Examination of the vertical structure of potential vorticity shows periods when at the highest levels studied (around 1800 K), the 4-day wave is responsible for the main motion of the vortex, while at lower levels (at and below ~1400 K) the vortex motion is characterized by a slower eastward progression) and the 4-day wave signal contributes to motions that are confined inside the vortex.

1. Introduction

Many observational and theoretical studies have focused on the 4-day eastward moving wave in the polar winter upper stratosphere and mesosphere. Allen et al. (1997) , give a review of such studies; the 4-clay wave is characterized by waves of zonal wavenumber 1 through at least 4, moving with the same phase speed, such that the wave 1 period is near 4 days. The 4-clay wave is observed in both hemispheres, although it is stronger in the southern hemisphere (e. g., Venne and Stanford 1982). Theoret ical studies (Manney and Randel 1993 and references therein) show that the observed characteristics of the 4-day wave are consistent with it originating through instability of the polar night jet in the upper stratosphere and lower mesosphere; many observed episodes of 4-day wave growth are consistent with primarily barotropic instability (e.g., little vertical phase tilt, poleward momentum flux), although some show evidence of the importance of both barotropic and baroclinic effects (e. g., equatorward momentum and heat flux, phase tilt with height) (e.g., Manney 1991; Randel and Lait 1991; Allen et al. 1997; and references therein).

Bowman and Chen (1994) and Orsolini and Simon (1995) studied the non-linear evolution of barotropically unstable modes including the 4-day wave and transport associated with these using idealized models. Bowman and Chen (1994) found that unstable modes poleward of the polar night jet produced weak mixing that was entirely confined to the vortex. Orsolini and Simon (1995) found extensive mixing within the vortex during wave growth, and mixing between the vortex and its edge during wave decay.

Allen et al. (1997) presented evidence of the 4-day wave in temperature, geopotential height and ozone data from the Upper Atmosphere Research Satellite (UARS) Microwave Limb Sounder (MLS) in the 1992 and 1993 late southern hemisphere (SH) winters, in the upper stratosphere and lower mesosphere. Other eastward moving wave features have also been ident ified in MLS temperat ure and ozone data in the 1992 late SH winter in the upper stratosphere (Fishbein et al. 1993) and Lahoz et al. (1996a) examined the evolution of the middle-stratospheric polar vortex during this period.

In the SH late winter of 1992, several other fields are available from UARS instruments, in particular water vapor (H_2O) from MLS and methane (CH_4) from the Cryogen Limb Array Etalon Spectrometer (CLAES). At levels below ~65 km, the chemical lifetimes of both H_2O and CH_4 are months to years (e. g., Brasseur and Solomon 1986), so their evolution on time-scales of days and weeks should be controlled primarily by transport. In the following we examine these fields for evidence of eastward-traveling waves, in particular, the 4-day wave. We use MLS H_20, CLAES CH_4 and idealized tracers to initialize isentropic transport calculations, allowing qualitative comparison of the calculated wave signatures due to horizontal transport processes with the observed 4-day wave signatures.

2. Data and Analysis

The MLS Version 31120 data and validation arc! described by Lahoz.al. (1996b). Both these and the Version 4 production retrievals of 11_20 showed puzzling behavior in the polar middle and upper stratosphere during winter periods including the late winter 1992 period that we are interested in here (e.g., Manney et al. 1995); this behavior appeared inconsistent with the expectation that the evolution of H_20 in the middle aud upper stratosphere is driven primarily by transport. The production retrievals of M S H_20 have several other known flaws, some due to the fact that the production retrieval is not iterative, some because of problems associated with the modeling of the instrument and atmosphere, and some because the production retrieval uses a coarse vertical grid. Recently, a prototype iterative retrieval has been developed at the University of Edinburgh's Department of Meteorology. This retrieval applies the optimal estimation equation once and then re-linearizes about the result before applying it again; the process is repeated until a convergence criterion is met. The iterative retrievals are described in more detail by Pumphrey (1997). The retrieved profiles are on the standard pressure grid for UARS L3 files, which is twice as fine as the grid used for MLS Version 3 and 4 retrievals. The vertical resolution of which the instrument is , capable is better in the middle stratosphere than the ~5 km MLS Version 4 grid, but not quite as good as the 2.5 km of the L3 grid; above ~1 mb the vertical resolution is rather worse, on the order of 6 or 7 km. Examination of the overall time evolution of H_20 retrieved this way for 14 Aug through 19 Sep 1992 shows behavior which appears more consistent with transport processes than the earlier retrievals. It is these H_20 data that we focus on here. Single profile precision for these data is estimated to be ~0.15- 0.35 ppmv between 10 and 0.1 hPa, with accuracy of ~0.7 to 0.9 ppmv.

We have also examined CLAES Version 7 CH_4 data, described by Roche et al. (1996); these have random errors of ~0.05-0.08 ppmv, and a systematic error of ~1 5%, with CLAES biased high with respect to correlative data. Version 8 CLAES CH_4 data are also available, but exhibit larger biases than Version 7 CH_4 data, resulting from known problems in the Version 8 retrieval algorithm. Analyses like those shown here using Version 8 CH_4 data show very similar results.

UARS data are interpolated to isentropic surfaces using temperatures from the UK Meteorological Office (UKMO) troposphere-stratospbcrc data assimilation system (Swinbank and O'Neill 1994), for comparison with isentropic transport calculations. Those spectral analyses that are being compared with transport calculations are performed using these interpolated fields. Once daily gridded H_2O and CH_4 data were obtained using a Fourier analysis procedure which separates longitude and time variations (Elson and Froidevaux 1993). An additional complication in the spectral analysis of CH_4 is that CLAES data iu the region of interest are missing for many orbits on 2 days (27 Aug and 1 Sep) during the period of study. The gridding procedure described above interpolates over missing data to produce complete gridded fields on each day. However, we have less confidence in the details of' the fields on those days when the majority of the data were missing, especially since rapid changes in the flow are occurring during the time period being studied.

The spectral analysis presented here uses the same methods described by , Manney (1991), who followed the methods described in more detail by Venne and Stanford (1982). For comparison with the transport calculations, we ate using 24-day time series; for these shorter time series, we use an 8-clay spectral window. As in Manney (1991), we present plots of the ratio of eastward-moving variance to noise variance (ES/N), large values of which indicate that the wave feature could be detected in the presence of noise. Since we are primarily interested in the 4-day wave (part of a quasi-nondispersive feature, only the wave 1 component of which can be reliably detected in once daily data), and since wavenumber 1 features are dominant in the middle and upper stratosphere at this time (e. g., Fishbein et ai. 1993), we focus here on wave 1. Figure 1 shows the ES/N at 1800 K($\sim$1 - 1.5 hPa) for analyses of UKMO temperatures and Version 4 MLS ozone. Although displayed differently, these results are in good agreement with those from ML S temperatures and Version 3 ML S ozone shown by Allen et al. (1997). Filtering is done in the frequency domain, as described by Manney (1991). Comparison of time-longitude (Hovmöller) plots of the 4-day wave in UKMO temperatures shows excellent agreement in 4-day wave amplitude and evolution with that shown by Allen et al. (1997). We have also done spectral analyses of UKMO winds and potential vorticity (PV) calculated from the UKMO data, and transport calculations initialized with UKMO PV.

The transport code is described by Orsolini (1995); the ability of this model to simulate high-resolution tracer fields and small-scale structure such as filamentation in those fields has previously been demonstrated [e. g., Orsolini et al. 1997 anti references therein). It is used here on a Gaussian T106 grid, giving $\sim$1 .125° resolution, and is run on individual isentropic surfaces that are of interest. The advecting winds are from the UKMO analyses, interpolated to the appropriate isentropic surfaces and the model grid. Since the calculations are isentropic, and since, in the polar middle and upper stratosphere at this time, diabatic descent rates are relatively large (e.g., Manney et al. 1994), we do not expect to quantitatively reproduce the observed fields with the transport calculations, but only to examine the ability of these calculations to reproduce the general features of the transport of the tracers by traveling planetary scale waves.

Transport calculations and spectral analyses are done for 24-day periods, starting on 14 Aug 1992 for calculations with MLS H_20, and on 17 Aug 1992 for CLAES CH_4; each starting date is the first complete clay on which data from that instrument are available at high southern latitudes in that observing period. For spectral analyses and Hovmöller plots, we have sampled the output of the transport calculations once daily at 12 UT, consistent with the observed fields.

3. **Results**

a. Overview

To first order, assuming linear wave theory, the amplitude of a wave in a passive tracer transported by horizontal motions goes as:

$$\mu'^2 \sim \frac{1}{k^2(\overline{u}-c)^2}\left[\left(\frac{\partial\overline{\mu}}{\partial y}\right)^2 v'^2\right]$$

where μ' and v' are the amplitudes of sinusoidally varying wave components of mixing ratio and meridional velocity, respectively, with wavenumber k and phase speed c (see, e.g., Allen et al. (1997), equations 8 and 9). Thus, we would expect to see waves amplify in the tracer field where $(\overline{u}$ – c) is small, the amplitude of the perturbation in the meridional velocity is large, and the zonal mean tracer mixing ratio exhibits significant meridional gradients. Figure 2 shows cross-sections of H_2O and CH_4 mixing ratios with contours of zonal mean wind overlaid, averaged over 4 days near the middle of the time period we are considering. In late winter the peak in MLS H_2O in the polar regions is near 2 hPa, and H_2O shows significant horizontal tracer gradients at high latitudes only above about 1.5 hPa. In contrast, CLAES CH_4 shows strong horizontal gradients at high latitudes only below about 2 hPa. The phase speed of a wave with a 4-clay period is about 40 m/s at 70°S and about 65 m/s at 55°S, so there are regions near these latitudes over a broad vertical range for which ($\bar{u}$ – c) is small. Figure 3 shows ES/N for UKMO meridional winds at 1800 and 1400 K, for time series beginning on 14 Aug and 17 Aug, respectively, indicating a strong signal with a period near 4 days and a double-peaked structure in latitude at 1800 K and a signal at 1400 K with a period near 4 days at high latitudes and somewhat longer periods (near 5-7 clays) at ~50°- *60°s.*

Figure 4 shows ES/N for H_2O and CH_4 at 72°S as a function of pressure, for time series beginning on 14 August ant] 17 August, respectively. As suggested by the above general arguments, H_2O shows a signal with a period near 4 clays at levels above about 1.5 hPa and CH_4 shows a signal with a period near 4 days at about 3 hPa, and longer period (5-1 O clays) signals below.

b. Water Vapor

The UKMO winds become somewhat noisy in the top few levels for which they are available, above about 1 hPa (Swinbank and O'Neill 1994). We therefore chose to run transport calculations initialized with 11_20 at 1800 K (~1.5 hPa at 800^s to 1 hPa at 50° S), which is the highest level for which we feel the winds are sufficiently reliable. Figure 5 compares ES/N for MLS H_2O at 1800 K with that for a transport calculation initialized with MLS H_2O on 14 Aug 1992. The observed 4-clay wave signal shows strong peaks near 72°S and 56°S. While the signal from the transport calculation shows much more latitudinal structure (recall that the transport calculation has ~1.125° resolution, as opposed to 4° for the gridded NILS data), there are distinct peaks near 72° and 56° S corresponding to those seen in the observations. At lower latitudes, the observed and calculated signals do not agree as well. A similar transport calculation was done for this period for an idealized tracer ("PV-tracer") whose initial mixing ratio was the UKMO PV at 1800 K on 14 Aug 1992; spectral analyses of UKMO PV and transported PV-tracer at 1800 K show ES/N patterns very similar to those seen in H_2O, with peaks of about 4-day periods at ~72°S and ~60°S.

Figure 6 compares time-longitude (Hovmöller) plots of wave 1, and wave 1 filtered for 2.9 6.4 d periods, for observed and transported H_2O at 1800 K. The overall agreement between the observed and calculated fields is fairly good near the beginning of the transport calculation (as expected) and after about 25 Aug 1992; the observed and calculated wave 1 phases agree well after 25 August, and a fast eastward-moving feature is readily apparent in the full wave 1 fields around 30 Aug- 1 Sep 1992, with a more slowly eastward-moving feature amplifying after that time. The filtered fields show good agreement in the 4-day wave features, in that the phase is nearly identical for each, and the time evolution is similar, with maximum amplitudes between about 25 and 30 Aug 1992, after which time amplitudes decrease slowly. The maximum amplitudes seen in the transport, calculation are similar to those observed. Comparison to Hovmöller plots of the 4-day wave in temperature (e. g., Allen et al. 1997) and meridional velocity shows that the 4-day wave in H_2O is 90° out of phase with the perturbation in meridional velocity and in phase with the temperature perturbation; this is consistent with the relationships found by Hartmann and Garcia (1979) for transport by planetary scale waves of a dynamically y-controlled tracer in a quasi-geostrophic model.

Figure 7 shows an eight-clay sequence of maps of observed and transported H_2O fields at 1800 K, for 29 August- 5 September. At the beginning of this period, the 4-day wave is the dominant feature (Figure 6); at the end of this period, the slowly moving and quasi-stationary wave 1 components amplify and are in phase around 5 September, leading to a very large total wave 1 amplitude (Fishbein et al. 1993). Although the appearance of the plots is somewhat different, due to the high resolution of the transport calculations and the low resolution of the observed fields, the full fields agree well in the general shape and position of the polar vortex, and in the tongues of high H_2O that are drawn up around the vortex (e. g., on 4 and 5 Sep 1992). Generally slightly higher H_2O in the transport calculations inside the vortex is consistent with the isentropic calculations, since at this time and level diabatic descent is strongest inside the vortex; since vertical H_20 gradients are also relatively strong there (Figure 2), lower H_20 is transported to this level by processes that were not included in the calculations. At this time and level, the 4-day wave is the strongest signal in the field; after this time, a more slowly moving wave 1 feature amplifies (e.g., Figure 6 and Fishbein et al. (1993)). During the first 5-6 days shown in Figure 7, when the 4-day wave is the dominant feature at this level, the, entire vortex rotates with an ~4-day period. At the end of this period (3- 5 September), the 4-day wave is still present, although its amplitude is decreasing (Figure 6); however, the amplifying slowly moving and quasi-stationary wave 1 features become. dominant.

Plots of the wave 1 component filtered for 2.9 6.4 day periods for the last 4 days of the period shown in Figure 7 (Figure 8) show a generally double-peaked structure in the 4-clay wave 1 field, with the phase agreeing very well at high latitudes, but somewhat less well as latitude decreases. The main feature of disagreement is the sudden phase change that is seen at about 50°S in the observed 4-day wave, which is largely absent in the transport calculations. At this latitude, however, the amplitude of the 4-clay wave is small in both calculated and observed fields, so this difference does not lead to a significant disagreement in the tracer fields.

c. Methane

Transport calculations for CH_4 were run at 1400 K and 1100 K, where zonal mean CH_4 shows strong gradients at high latitudes (Figure 2) and there were significant wave 1 signals at 72°S (Figure 4). Figure 9 compares spectral analyses for observed and calculated CH_4 at 1400 K. Although there arc some regions of disagreement (particularly near 50°S), both fields show signals with periods near 5-10 days at latitudes from about 76°S to 60°S, a very slowly moving signal south of ~72°S, and a signal with ~4-day period near 70°S. Analyses of CH_4 and transported CH_4 at 1100 K show very similar , features, but with a stronger slowly moving wave 1 signal, and less 4-day wave signal. Figure 10 shows Hovmöller plots of the complete wave 1 field in CH_4 at 1400 K and 72°S, and wave 1 filtered for 2.9- 6.4 day periods, from observations and calculations. The strong slowly moving wave 1 signal that amplifies after about 2 September is apparent in both fields, with the same phase and approximately the same period. Figure 10 shows that the phase and amplitude of the 4-day wave agree well between calculations and observations, but the transported 4-day wave in CH_4 amplifies slightly later than the observed feature. As was the case with H_2O at 1800 K, spectral analyses and Hovmöller plots of PV at 1400 K show very similar signals to those in (311$_4$.

Figure 11 shows Hovmöller plots of wave 1 at 1100 K and 68°S in observed and transported CH_4. At this latitude and level, the small amplification of the slowly moving wave 1 near 25 August noted by Fishbein et al. (1993) is apparent, as well as the large wave 1 amplification event near 5 September. Figures 9, 10 and 11 all indicate a stronger stationary or very slowly moving wave 1 component in the transport calculations than in the observations.

Figure 12 shows a sequence of maps of CLAES CH_4 at 1400 K from observations and calculations for 2-5 September (the last 4 days shown for H_2O at 1800 K in Figure 7, days chosen to be after those for which CLAES data were missing), showing good agreement in the shape and position of the vortex. Overall higher values for material that is drawn up around the vortex in the transport calculation are probably due to the absence of diabatic descent in that calculation, since diabatic descent is strong at this time, and tends to be strongest along the vortex edge on the side where material is being drawn up (e.g., Manney et al. 1994). Inspection of diabatic heating rates shows strong descent in the center of the vortex (where vertical CH_4 gradients are weak, as shown in Figure 2) and outside the vortex on the side where high CH_4 is drawn up (where vertical CH_4 gradients are strong, as shown in Figure 2). This pattern with greater differences between observations and calculations in the regions of high CH_4 , probably contributes to the appearance of larger wave 1 amplitudes in the calculations. In contrast to the pattern at 1800 K in H_2O (Figure 7), the vortex is larger at 1400 K and the rotation of the vortex itself has a long period, ~10-15 clays. A faster rotation of the material within the vortex can be seen in the maps from the transport calculations (and, albeit less clearly, in the observed maps) during the first three days shown here. The slowly-moving wave 1 is amplifying at the end of this period, and becomes the dominant signal over all high latitudes.

Figure 13 shows similar maps of CH_4, but at 1100 K. The overall behavior is very similar to that at 1400 K, with rapidly rotating material inside a more slowly moving vortex. The slowly moving wave 1 is weaker at this level on 2 September, and builds up gradually. Comparison of Figures 12 and 13 thus shows a westward and equatorward tilt of the vortex with height during the amplification of the slowly moving wave 1 feature. Comparison with Figure 7 shows, most noticeably in the transport calculations on 2 and 3 September, that the smaller rapidly moving vortex at 1800 K is approximately in phase with the rapidly moving material in the inner vortex at the lower levels; that is, the 4-clay wave during this period does not show a phase tilt with height. As the slowly moving wave 1 amplifies (e.g., 3 September), we see the westward and equatorward tilt of the vortex extend up through 1800 K. At 1100 K, the intensification of the anticyclone discussed by Lahoz et al. (1996a) can be clearly seen, and the coiling of material in the anticyclone is apparent in the transport calculations. As noted by Lahoz et al. (1996a), this anticyclone progresses eastward, with the eastward progression slowing and its intensity decreasing as it reaches the dateline.

d. Discussion

Because, as is apparent in Figure 2, the structure of the tracers H_2O and CH_4 is such that a strong signal from transport by eastward moving waves is expected (and appears, Figure. 4) only over a limited range of levels, it is somewhat difficult to get a clear picture of the three-dimensional structure of the wave motions. To clarify this, we look at the observed evolution of UKMO PV; as noted above, spectral analyses of PV and transported PV-tracer show very similar signals to those of H_2O and CH_4, but since PV has strong horizontal gradients over the entire range of attitudes shown, all of the features discussed above can be seen in PV. We show the three-dimensional evolution of the wave features by presenting fields of PV scaled in "vorticity units" (e. g., Dunkerton and Delisi 1986) as described in detail by Manney et al. (1994), so as to have a similar range of values at all levels. Figure 14 shows a six-clay sequence of the departure of scaled PV from the zonal mean, as a function of potential temperature, around the 72°S longitude circle, with the wave 1 component of this eddy indicated in the background. As can be seen from Figures 7, 12 and 13, this cuts through the vortex edge at the highest levels shown, and through the inner vortex material at the lower levels. An approximately 4-day motion of wave 1 can be seen at all levels above ~900 K in the first five days shown. This motion is the dominant signal at the highest levels at the end of August, as is apparent from comparing the wave 1 and full eddy fields (although there are significant features at higher wavenumbers). At the lowest levels shown, a slowly moving or stationary wave 1 is the strongest feature throughout the period; this feature only becomes obvious at the highest levels in the last few days shown.

Figure 15 shows isosurfaces of the 1.2 x $10^{-4}\,s^{-1}$ scaled PV contour for the same six days. In contrast to Figure 1-1, which showed the evolution along a latitude circle, this shows approximately the evolution of the vortex, since at all levels shown the 1.2 $\times\ 10^{-4}\ s^{-1}$ contour is in the region of strong PV gradients demarking the vortex edge. We can see more clearly here that, at the top, the entire vortex (which has already been eroded to some degree at these levels, and is thus smaller and weaker than the mid-winter upper stratospheric vortex (e. g., Manney et al. 1994)) rotates with a 4-day period, while at the lower levels it is nearly stationary. Fishbein et al. (1993) showed ~10-day and quasi-stationary wave 1 features interfering constructively near 25 August and 5 September, leading to a small amplification of wave 1 around 25 August and a large amplification around 5 September. The first of these events can been seen in in Hovmöller plots of CH_4 at 1100 K (Figure 11). The large wave 1 amplification around 5 September is seen at levels throughout the stratosphere. At 1800 K, the 4-clay wave existed prior to the first of these amplifications (Figure 6) and comprises at least four cycles. The 4-clay rotation around the pole appears clearly before about 3 September and is not masked by the displacement of the vortex off the pole clue to slowly moving waves associated with anticyclogenesis (Figures 6, 7, 14 and 15). The large wave 1 amplification near 5 September is linked to the genesis of a strong anticyclone, as shown by Lahoz et al. (1996). By about 3 September, this anticyclone spans the range of levels studied; it propagates slowly eastward (Figures 7, 12 and 13), and decays as it reaches the dateline (Figures 6, 10 and 11; Lahoz et al. (1996a)).

The behavior of PV shown in Figures 14 and 15 demonstrates more clearly the evolution that is apparent in the tracers 11_20 and CH_4. At the highest levels studied, where the late winter vortex has been somewhat eroded and is relatively small, the entire vortex rotates with a 4-day period at the time of maximum 4-day wave amplitude, while at lower levels, the 4-day motion is confined within the vortex. Bowman and Chen (1994) and Orsolini and Simon (1995) found, in idealized studies of transport by barotropically unstable waves like the 4-day wave, that mixing by these waves was in general confined inside the polar vortex. Their results appear qualitatively similar to the situation we have sccu at the lower levels. Since their simulations were for strong, midwinter-like vortices, our results from observations and transport calculations using observed winds appear to confirm those results showing that the effects of transport by the 4-day wave were confined within the vortex. In contrast, we have seen that at 1800 K the entire vortex rotates with a 4-day period, and further examination of observed and transported $11_2$0 maps such as those in Figure 7 indicates that during the time when the 4-day wave is dominant, material is being drawn off the vortex edge and mixed into mid-latitudes. This type of behavior has not been seen in idealized simulations (although Orsolini auct Simon (1995) showed some mixing between the vortex and its edge during wave decay). This is probably because situations with a small and somewhat weakened vortex such as that at 1800 K in late austral winter 1992 have not been examined. In addition, the observed and simulated behavior shown here, in the presence of other wave features, exhibits a degree of complexity that would not be expected in simulations of the 4-clay wave in isolation.

The 4-day wave is generally thought to originate via instability (e.g., Manney and Randel 1994 and references therein), in many cases primarily barotropic instability. Allen et al. (1997) showed that the necessary conditions for instability were indeed fulfilled during the time period studied here. Their results, the confinement of the 4-clay wave to the upper stratosphere aud lower mesosphere (as noted in previous studies), ancl the lack of phase tilt with height of the 4-clay wave shown here suggest that in this period the mechanism is primarily barotropic instability. However, as shown above, the situatiou during this period is never that of a simple unstable wave growing on a zonally-symmetric basic state. As well as the slowly moving and quasi-stationary wave 1 features discussed above, a relatively strong, slowly eastward-moving wave 2 amplified around 23 August and 3 September (although its amplitude was newer over about half the maximum reached by wave 1); this type of wave 2 feature is common in the austral late winter and spring (e.g., Manney et al. 1991). Manney ct al. (1989) showed that the presence of waves resembling those typically observed in the stratosphere could have a marked effect on the stability of the stratospheric polar night jet. In particular, they found that, while a slowly moving or stationary wave 1 did not materially affect the stability of modes resembling the 4-day wave, a slowly eastward-moving wave 2 of very modest amplitude could in fact considerably destabilize such modes. They also found that if a mode resembling the 4-day wave were already present, it could lead to further amplification of quasi-nondispersive features moving with the same phase speeds. We can see (Figures 6 and 10) that the 4-clay wave amplified earlier at higher altitudes; resonant type behavior such as that found in the theoretical studies of Manney et al. (1989) could contribute to the subsequent amplification at lower altitudes. Because of the variety of wave activity present during August and September 1992, such considerations are undoubtedly important in determining the observed life-cycle of the 4-clay wave.

4. Summary

We have examined UARS tracer data and isentropic transport calculations initialized with these data for evidence of eastward-traveling waves in the polar upper stratosphere in late Austral winter 1992. Spectral analyses of MLS H_2O from prototype iterative retrievals indicate a 4-clay wave signal in H_2O, at levels from ~1 .5- 0.1 hPa. At levels below ~1.5 hPa, horizontal H_2O gradients are weak in high latitudes, so a signal that is produced mainly by horizontal transport would not be expected. The 4-clay wave in H_20 at, 1800 K (~1-1.5 hPa) has a double-peaked structure in latitude, with maximum amplitudes near 72°S and 56° S. A 4-day wave signal was not obvious in production retrievals of MLS H_2O. Isentropic transport calculations initialized with MLS H_2O reproduce a double-peaked structure, with maxima at approximately the same latitudes. The time evolution, amplitude and phase of the 4-day wave in the transport calculations agree well with those in observations at high-latitudes. Equatorward of ~50° S, the? observation show a sudden phase change which is not reproduced in the calc ulat ions; this occurs, however, at, a latitude where the 4-day wave amplitude is small. The overall qualitative agreement between the full H_2O fields in calc ulat ions and observations at 1800 K is good, with the position and shape of the polar vortex and of tongues of higher H_2O drawn up around the vortex reproduced by the calculations.

CLAES CH_4 observations show strong horizontal gradients at high latitudes below ~2 hPa, and spectral analysis of CH_4 shows a 4-day wave feature between ~4 and 2 hPa and eastward-traveling wave features with periods of 5-10 clays below about 3 hPa. Transport calculations initialized with CH_4 show a similar eastward-traveling signal, with good agreement between the phase of observed and calculated fields. The transport calculations show a stronger stationary component than the observed CH_4, and, as in H_20, disagreement at lower latitudes where fast-moving wave amplitudes are small. There is agreement of the position of the vortex and of tongues of high CH_4 drawn up around the vortex in observed and transported fields.

Several factors may influence the lack of quantitative agreement between observations and calculations. Diabatic descent rates are relatively large in the polar middle and upper stratosphere at this time, so the inclusion of only horizontal motions in the transport calculations leads us to expect some differences. Also, the coarse horizontal resolution of the observed fields leads to differences in detail, as small or narrow features seen in the transport calculations, even were they present in the real atmosphere, might be missed by the sampling pattern of the satellite instruments. Different relatively small scale features will be sampled by the satellite instruments on different days, depending on their location with respect to the sampling pattern; thus, the NILS and CLAES initialization fields may include some, but not all, of the relatively small-scale structure that is present in the atmosphere. Finally, in any transport calculation, the accuracy of the advecting winds is problematic and difficult to assess quantitatively. Sonic previous transport calculations using UKMO winds show agreement between observe{] and calculated tracers that is relatively poor in mid-latitudes (outside the vortex, away from its edge) (e. g., Manney et al. 1995).

Despite some points of disagreement between observed and calculated fields, the transport calculations were successful in qualitatively reproducing the phase and time evolution of high-latitude eastward-traveling waves in the polar upper stratosphere in late southern winter 1992. This success indicates that the UKMO winds used for the transport calculations are generally reliable in this region, anti that the eastward-traveling wave features identified in the MLS H_20 and CLAES CH_4 originate to a large extent from horizontal transport processes.

The observed and transported tracer fields at the various levels studied show three-dimensional evolution of the 4-day wave in relation to the polar vortex that is consistent with the evolution of PV at this time. At the highest levels, near 1800 K, the vortex is small and weakened in late winter, and the entire vortex rotates with a 4-day period at the peak of the 4-day wave amplitude; at 1800 K, material is drawn off the vortex edge and mixed into mid-latitudes during this period, suggesting that the 4-day wave in this situation is an important factor in vortex/extra-vortex mixing. At lower levels (∼1 400 K and below), the 4-day rotation is confined to material in the inner part of a large, strong vortex, which rotates with a much slower period.

Acknowledgments. Thanks to the MLS and CLAES teams for their efforts iu making the data available, the UKMO (R. Swinbank, A. O'Neill) for meteorological data, Drs. I,. S. Elson and R. P. Thurstans for asynoptic mapping of MLS and CLAES data, and Dr. M. 1,. Santee for CLAES data examination aud helpful discussion, Part of this work was carried out while Y. J. Orsolini was a visiting scientist at Centre National de Recherches Météorologiques. Work at The University of Edinburgh (H. C. Pumphrey) was supported by the Natural Environ ment Research Council (NERC). Work at the Jet Propulsion Laboratory, California Institute of Technology and at the Lockheed Martin Palo Alto Laboratory was done under contract with the National Aeronautics and Space Administration.

References

Allen, D. R., J. L. Stanford, L,. S. Elson, E. F. Fishbeiu, L. Froidevaux, aud J. W. Waters, 1997: The 4-clay wave as observed from the Upper Atmosphere Research Satellite Microwave Limb Sounder. *J. Atmos. Sci.*, 54, 420-434.

Bowman, K. P., and P. Chen, 1994: Mixing by barotropic instability in a nonlinear model. *J. Atmos. Sci.*, 51, 3692-3705.

Brasseur, G., and S. Solomon, 1986: *Aeronomy of the Middle Atmosphere,* 2nd Edition, Reidel, Dordecht, 441 pp.

Dunkerton, T. J., and D. P. Delisi, 1986: Evolution of potential vorticity in the winter stratosphere of January-February 1979. *J. Geophys. Res.*, 91, 1199-1208.

Elson, L. S., and L. Froidevaux, 1993: The use of Fourier t ransforms for asynopt ic mapping: Early results from the Upper Atmosphere Research Satellite Microwave Limb Sounder. *J. Geophys. Res.*, 98, 23,039-23,049.

Fishbein, E. F., L. S. Elson. I,. Froidevaux, G. 1,. Manney, W. G. Read, J. W. Waters, and R. W. Zurek, 1993: MLS observations of stratospheric waves in temperature and ozone during the 1992 southern winter. *Geophys. Res. Lett.*, 20, 1255-1258.

Hartmann, D. L., and R. R. Garcia, 1979: A mechanistic model of ozone transport by planetary waves in the stratosphere. *J. Atmos. Sci.*, 36, 350-364.

Lahoz, W. A., A. O'Neill, A. Heaps, V. 1). Pope, R. Swinbank, R. S. Harwood, L,. Froidevaux, W. G. Read, J. W. Waters, and G. E. Peckham, 1996a: Vortex dynamics and the evolution of water vapour in the stratosphere of the southern hemisphere. *Q. J. R. Meteorol. Sot.*, 122, 423-450.

Lahoz, W. A., et al., 19! Mb: Validation of UARS Microwave Limb Sounder 183 GHz H_2O measurements. *J. Geophys. Res.*, 101, 10,129- 10,149.

Manney, G. L., 1. R. Nathan, and J. L. Stanford, 1989: Barotropic instability of basic states with a realistic jet and a wave. *J. Atmos. Sci.*, 46, 1250-1273.

Manney, G. I,., 1991: The stratospheric 4-day wave in NMC data. J. *Atmos. Sci.*, 48, 1798-1811.

Manney, G. L., J. D. Farrara, aud C. R. Mechoso, 1991: The behavior of wave 2 in the Southern Hemisphere stratosphere during late winter and early spring. *J. .4 tmos. Sci.*, 48, 976-998.

Manney, G. L., and W. J. Randel, 1993: Instability at the winter stratopause: A mechanism for the 4-day wave. *J. Atmos. Sci.*, 50, 3928-2928.

Manney, G. L., R. W. Zurek, A. O'Neill, and R. Swinbank, 1994: On the motion of air through the stratospheric polar vortex. *J. A tmos. Sci.*, 51, 2973-2994.

Manney, G. L., R. W. Zurek, W. A. Lahoz, R. S. Harwood, J. C. Gille, J. B. Kumer, J. I,. Mergenthaler, A. E. Roche, A. O'Neill, R. Swinbank, and J. W. Waters, 1995: Lagrangian transport calculations using UARS data. Part I: Passive tracers. *J. Atmos. Sci.*, 52, 3049-3068.

Orsolini, Y. J., 1995: On the formation of ozone laminae at the edge of the Arctic polar vortex. Q. *J. R. Meteorol. Sot., 121, 1923-1941.*

Orsolini, Y. J., aud P. Simon, 1995: Idealized life cycles of planetary-scale barotropic waves in the middle atmosphere. *J. Atmos. Sci.*, 52, 3817-3835.

Orsolini, Y., G. Hansen, U. Hoppe, G. Manney and K. Fricke, 1997: Dynamical modelling of wintertime Lidar observations in the Arctic: ozone laminae, and ozone depletion. Q. *J. R. Meteorol. Sot.*, **123**, 785-800.

Pumphrey, H. C., 1997: Nonlinear retrievals of water vapour from the UARS Microwave Limb Sounder (MLS). *Adv. Sp. Res.*, accepted.

Randel, W. J., and L. R. Lait, 1991: Dynamics of the 4-day wave in the Southern Hemisphere polar stratosphere. *J. A tmos. Sci.*, 48, 2496-2508.

Roche, A. E., et al., 1996: Validation of CH_4 and N_2O measurements by the Cryogen Limb Array Etalon Spectrometer instrument on the Upper Atmosphere Research Satellite. *J. Geophys. Res.*, **101**, 9679-9710.

Swinbank, R., aud A. O'Neill, 1994: A Stratosphere-troposphere data assimilation system. *Mon. Weather Rev.*, 122, 686-702.

Venne, D. E., and J. I,. Stanford, 1982: An observational study of high-latitude stratospheric planetary waves in winter. *J. Atmos. Sci.*, 39, 1026-1034.

Figure 1. Eastward moving signal-to-noise ratio (the ratio of eastward-moving variance to noise variance, ES/N) from 24-clay time series of UKMO temperature and Version 4 MLS ozone beginning on 14 Aug 1992, both interpolated to the 1800 K isentropic surface. The light and dark shading shows the coherence squared at the 95% and 99% confidence levels, respectively.

Figure 2. Zonal-mean, time-mean MLS H_2O (top) and CLAES CH_4 (bottom) for 28-31 Aug 1992, with contours of UKMO zonal wind overlaid.

Figure 3. ES/N for 24-day time series of UKMO meridional wind, at 1800 K beginning on 14 Aug 1992 (top) and at 1400 K beginning on 17 Aug 1992 (bottom). Shading is as in Figure 1.

Figure 4. ES/N at 72°S for 24-day time series of MLS H_2O beginning on 14 Aug 1992 (top) and CLAES CH_4 beginning on 17 Aug 1992 (bottom). Shading is as in Figure 1.

Figure 5. ES/N at 1800 K for 24-day time series beginning on 14 Aug 1992 of observed MLS H_2O (top) and H_2O from a transport calculation initialized with MLS H_2O on 14 Aug 1992 (bottom). Shading is as in Figure 1.

Figure 6. Time-longitude (Hovmöller) plots at 72° S of wave 1 in H_2O from MLS observations (left) and transport calculations (right), showing total wave 1 field (top) and wave 1 filtered for 2.9 6.4 day periods (bottom). Contour interval on top is 0.05 ppmv, on bottom, 0.016 ppmv. Negative values are shaded.

Figure 7. Maps of H_2O (ppmv) at 1800 K for 29 Aug-5 Sep 1992 from MLS observations (top) and transport calculations (bottom). The projection is orthographic, with 0° longitude at the top and 90°E to the right; the outer edge is at 46° S, with dashed lines every 10° latitude and longitude. Contour interval is 0.1 ppmv, with dark shading from 4.8 5.6 ppmv and light shading from 5.7 6.5 ppmv.

Figure 8. Maps of wave 1 in H_2O (ppmv) filtered for 2.9 6.4 day periods at 1800 K for 2-5 Sep 1992 (the last four days shown in Figure 7) from MLS observation (top) and transport calculations (bottom). Layout is as in Figure 7. Negative values are shaded.

Figure 9. ES/N at 1400 K for 24-day time series beginning on 17 Aug 1992 of observed CLAES CH_4 (top) and CH_4 from a transport calculation initialized with CLAES CH_4 on 17 Aug 1992 (bottom). Shading is as in Figure 1.

Figure 10. Time-longitude (Hovmöller) plots at 1400 K and 72°S of wave 1 in CH_4 from CLAES observations (left) and transport calculations (right), showing total wave 1 field (top) and wave 1 filtered for 2.9- 6.4 day periods (bottom). Contour interval on top is 0.036 ppmv, on bottom, 0.010 ppmv. Negative values are shaded.

Figure 11. Time-longitude (Hovmöller) plots at 1100 K and 68° S of wave 1 in CH_4 from CLAES observations (left) and transport calculations (right). Contour interval is 0.04 ppmv. Negative values are shaded.

Figure 12. Maps of CH_4 (ppmv) at 1400 K for 2-5 Sep 1992 from CLAES observations (top) and transport calculations (bottom). Layout is as in Figure 7. Contour interval is 0.05 ppmv, with dark shading from 0.2-0.45 ppmv and light shading from 0.75- 1.3 ppmv.

Figure 13. As in Figure 11, but at 1100 K. Contour interval is 0.08 ppmv, with dark shading is from 0.2-0.56 ppmv and light shading from 0.96 1.6 ppmv.

Figure 14. Cross-sections as a function of potential temperature around 72°S of the departure of scaled PV (calculated from UKMO data) from the zonal mean (contours), for 28 Aug- 2 Sep 1992. Contour interval is $0.1 \times 10^{-4}\ s^{-1}$; dashed lines indicate negative values. In the Background is the wave 1 component of the eddy, with a $0.25 \times 10^{-4}\ s^{-1}$ contour interval, and light grey and white representing negative values.

Figure 15. Time sequence of the 1.2 x 1(1¯” s¯1 isosurface of UKMO PV for 28 Aug 2 Sep 1992, shown from 1100 to 1900 K.

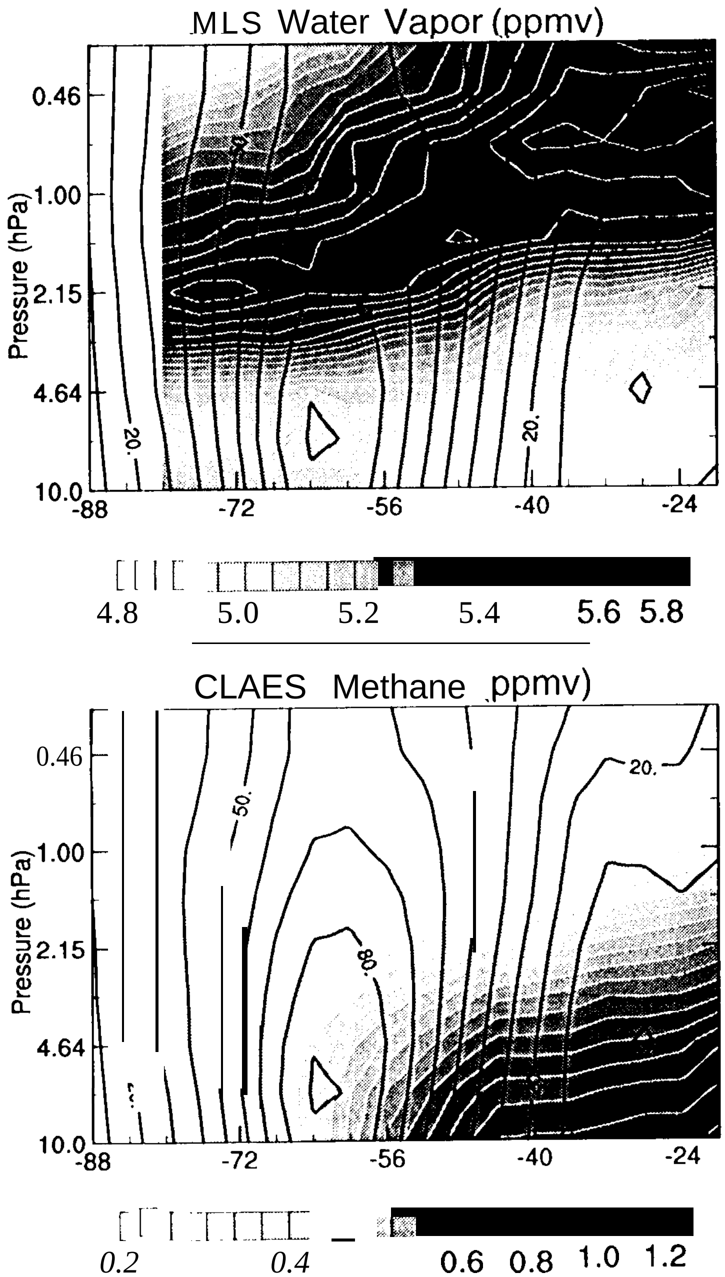

MLS Water Vapor (ppmv)
Pressure (hPa)
0.46
1.00
2.15
4.64
10.0
-88
-72
-56
-40
-24
50.
20.
20.
4.8
5.0
5.2
5.4
5.6
5.8
CLAES Methane ppmv)
Pressure (hPa)
0.46
1.00
2.15
4.64
10.0
-88
-72
-56
-40
-24
50.
80.
20.
0.2
0.4
0.6
0.8
1.0
1.2

Fig. 2

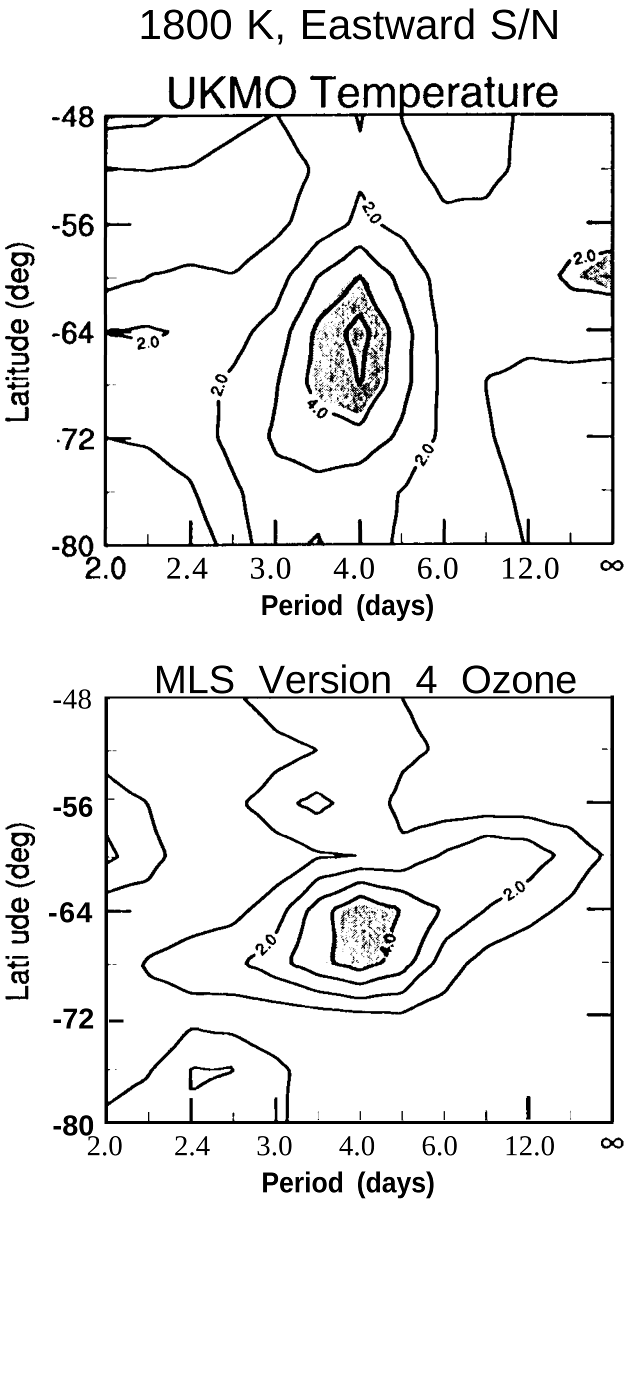
1800 K, Eastward S/N
UKMO Temperature
Latitude (deg)
-48
-56
-64
-72
-80
2.0
4.0
2.0
2.4
3.0
4.0
6.0
12.0
∞
Period (days)
MLS Version 4 Ozone
Lati ude (deg)
-48
-56
-64
-72
-80
2.0
4.0
2.0
2.4
3.0
4.0
6.0
12.0
∞
Period (days)

Fig. 1

Eastward S/N, 72 S

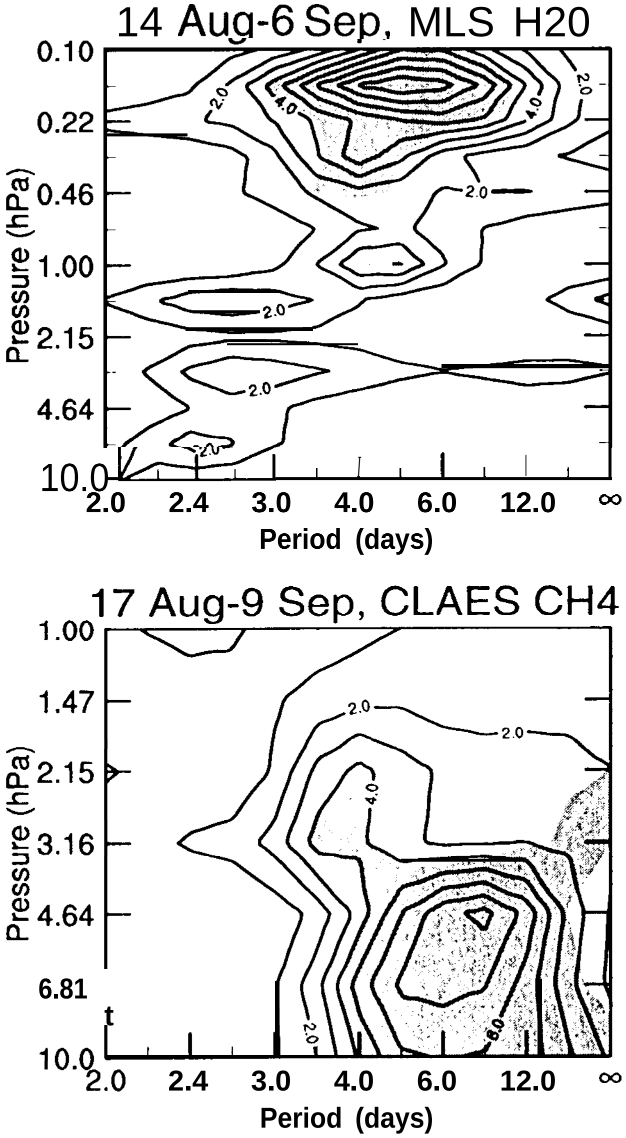

Fig. 4

UKMO Meridional Wind
Eastward S/N

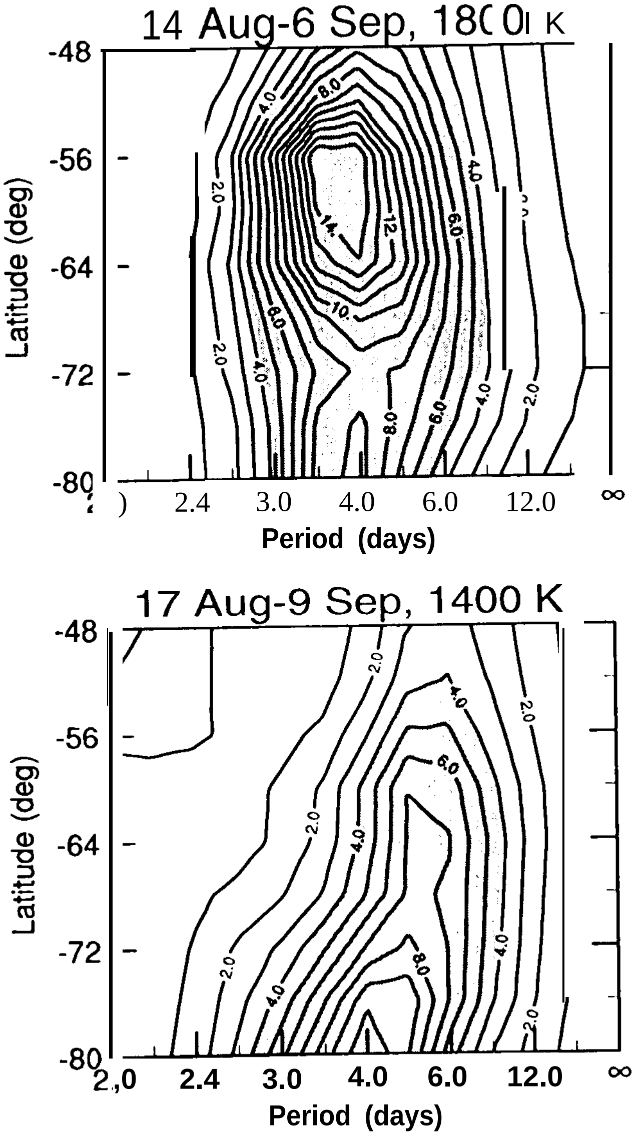

Fig. 3

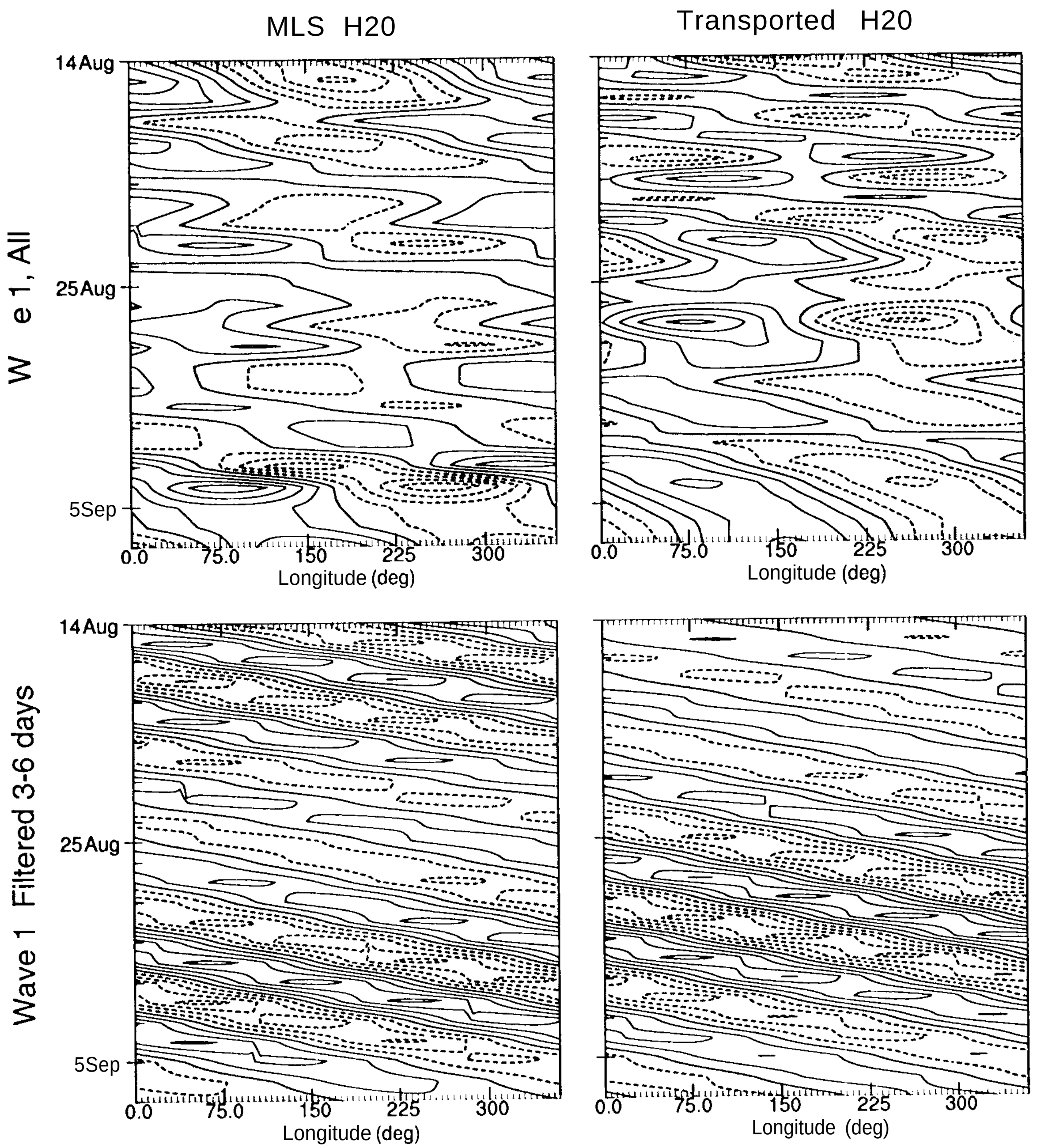
MLS H20
Transported H20
W e 1, All
Wave 1 Filtered 3-6 days
14 Aug
25 Aug
5Sep
0.0
75.0
150
225
300
Longitude (deg)

Fig. 6

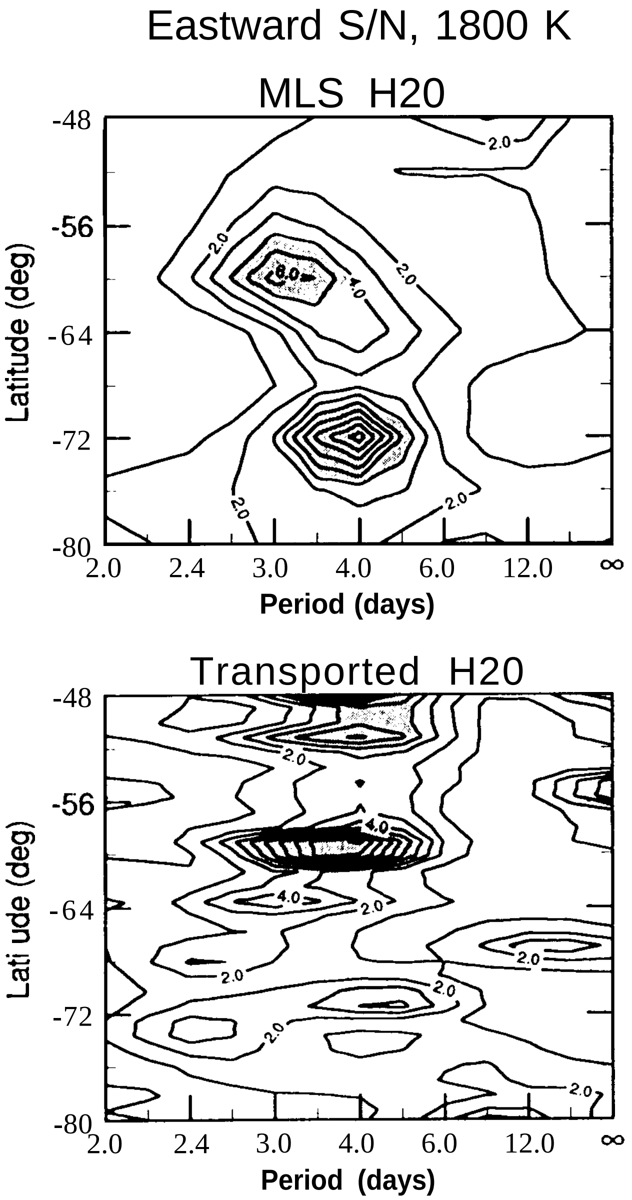
Eastward S/N, 1800 K
MLS H20
-48
-56
-64
-72
-80
Latitude (deg)
2.0
4.0
6.0
2.0
2.4
3.0
4.0
6.0
12.0
∞
Period (days)
Transported H20
-48
-56
-64
-72
-80
Lati ude (deg)
2.0
4.0
2.0
2.4
3.0
4.0
6.0
12.0
∞
Period (days)

Fig. 5

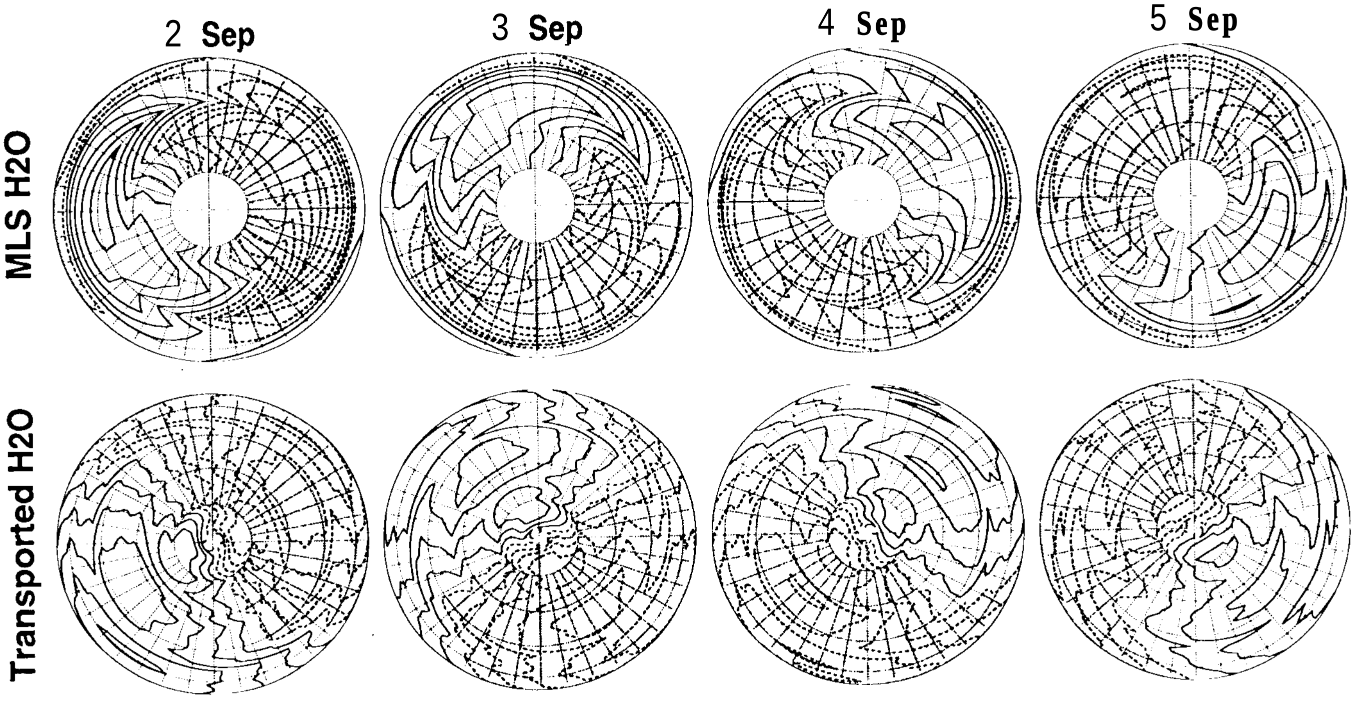

Fig. 8

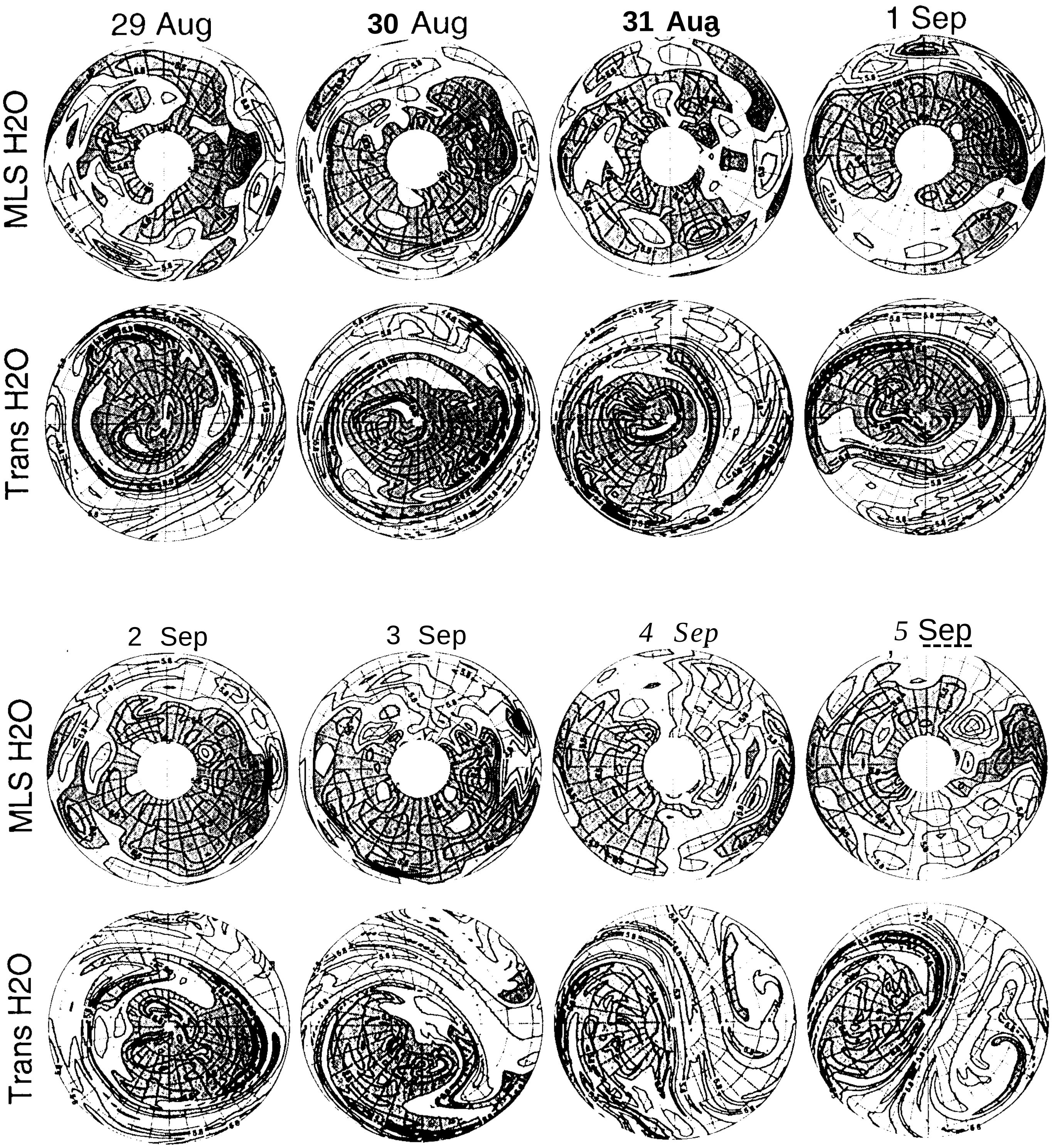
29 Aug
30 Aug
31 Aug
1 Sep
MLS H2O
Trans H2O
2 Sep
3 Sep
4 Sep
5 Sep
MLS H2O
Trans H2O

Fig. 7

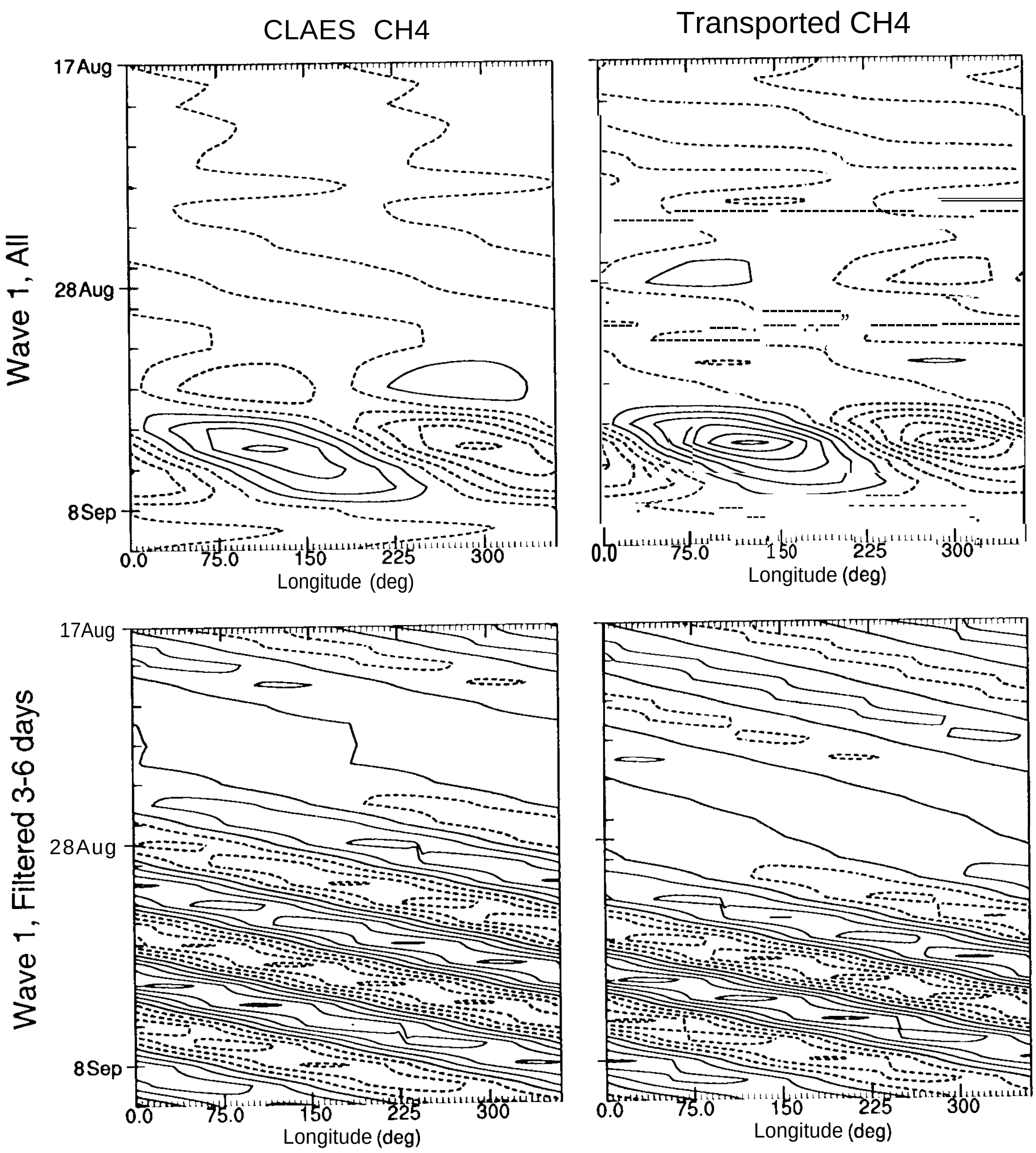

CLAES CH4
Transported CH4
Wave 1, All
Wave 1, Filtered 3-6 days
17Aug
28Aug
8Sep
0.0
75.0
150
225
300
Longitude (deg)

Fig. 10

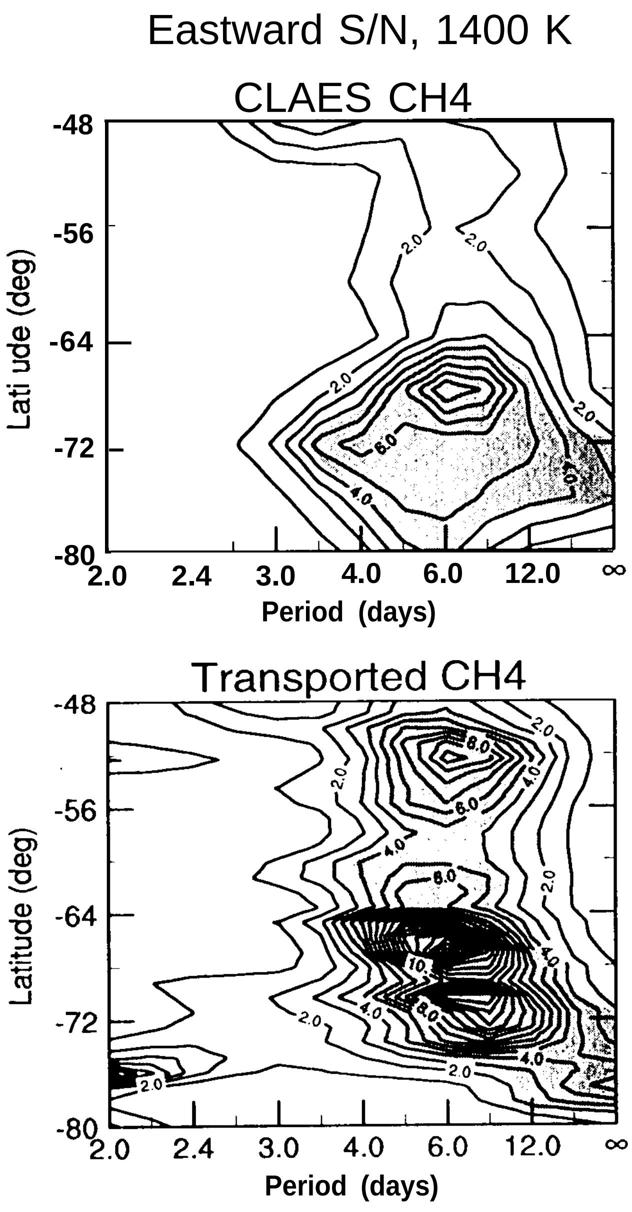

Eastward S/N, 1400 K
CLAES CH4
-48
-56
-64
-72
-80
Lati ude (deg)
2.0
2.4
3.0
4.0
6.0
12.0
∞
Period (days)
Transported CH4
-48
-56
-64
-72
-80
Latitude (deg)
2.0
2.4
3.0
4.0
6.0
12.0
∞
Period (days)

Fig. 9

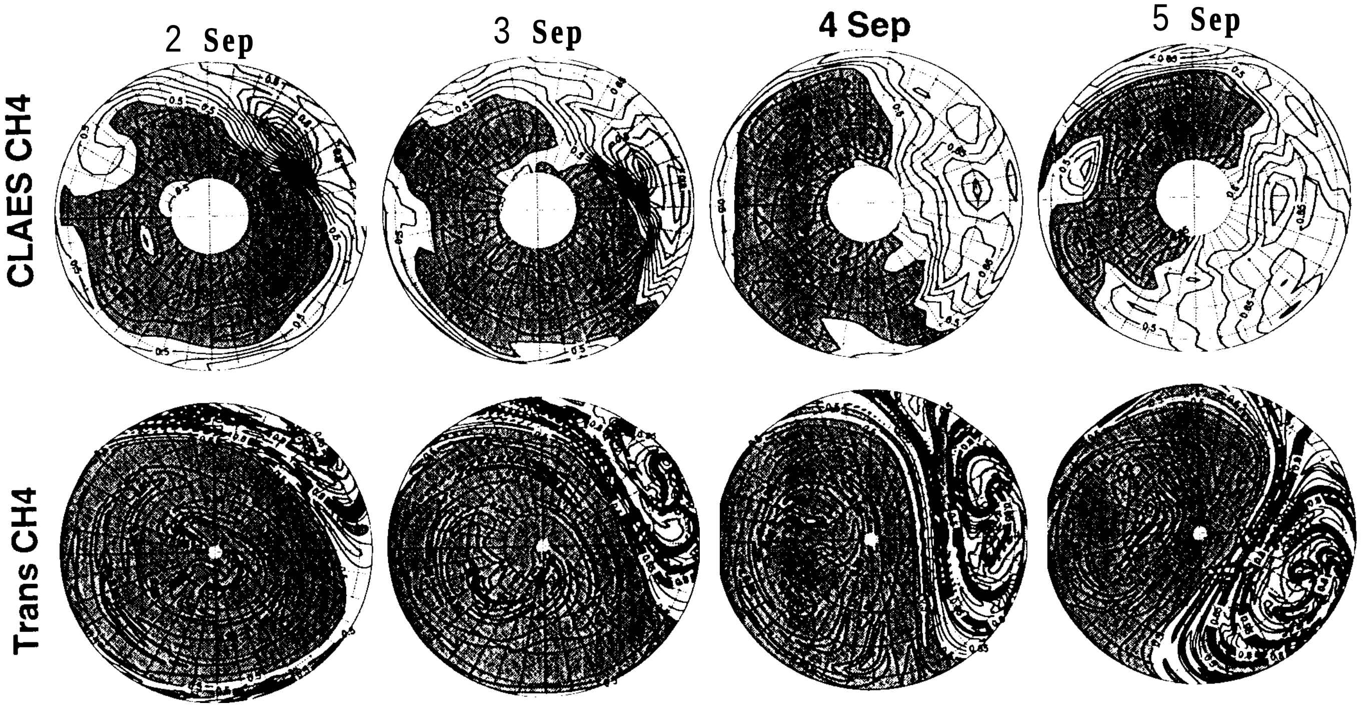

Fig. 12

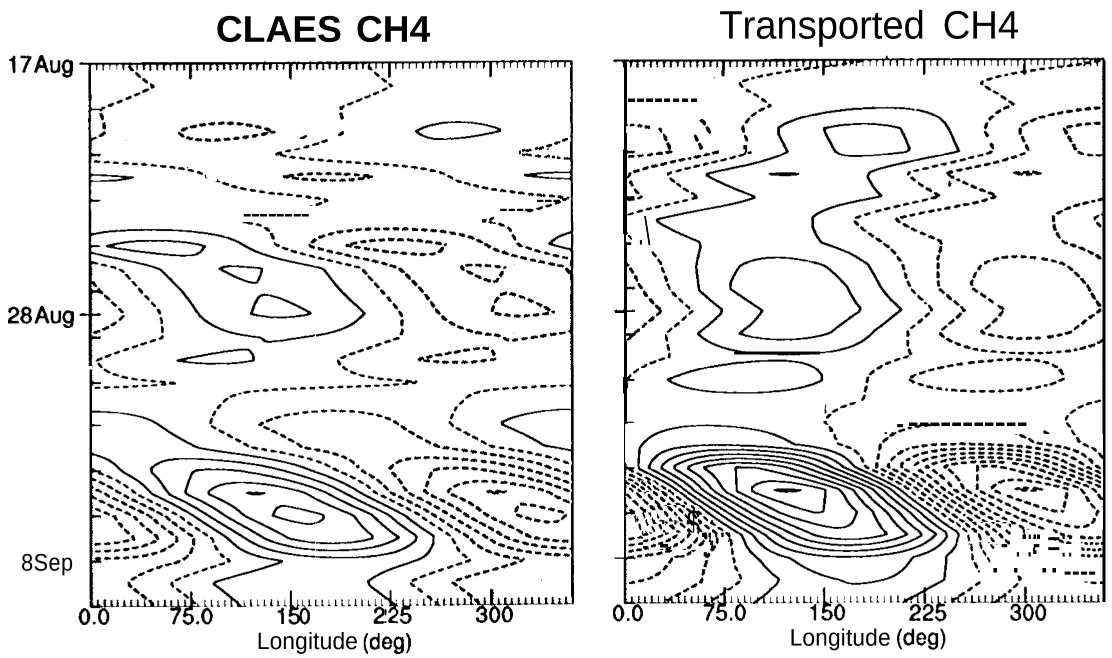

CLAES CH4
Transported CH4
17Aug
28Aug
8Sep
0.0
75.0
150
225
300
Longitude (deg)

Fig. 11

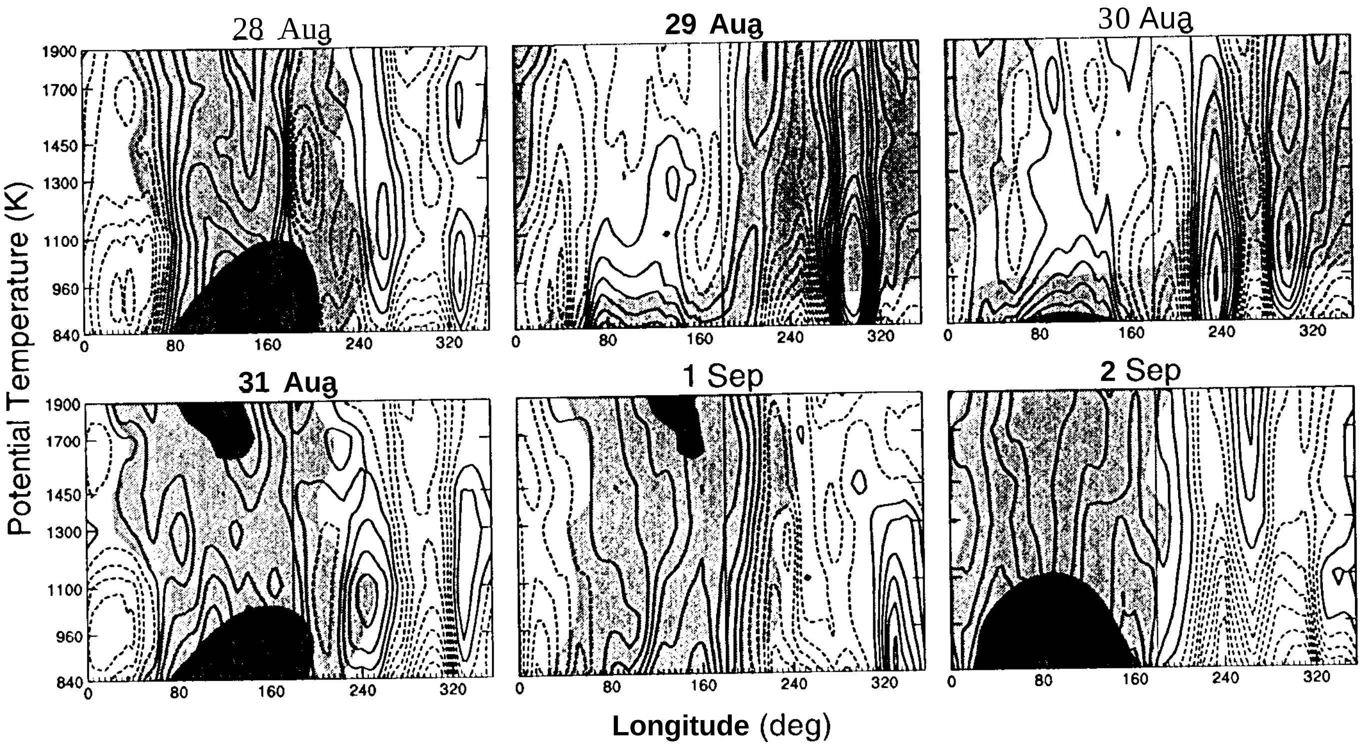
28 Aug
29 Aug
30 Aug
31 Aug
1 Sep
2 Sep
Potential Temperature (K)
1900
1700
1450
1300
1100
960
840
0
80
160
240
320
Longitude (deg)

Fig. 14

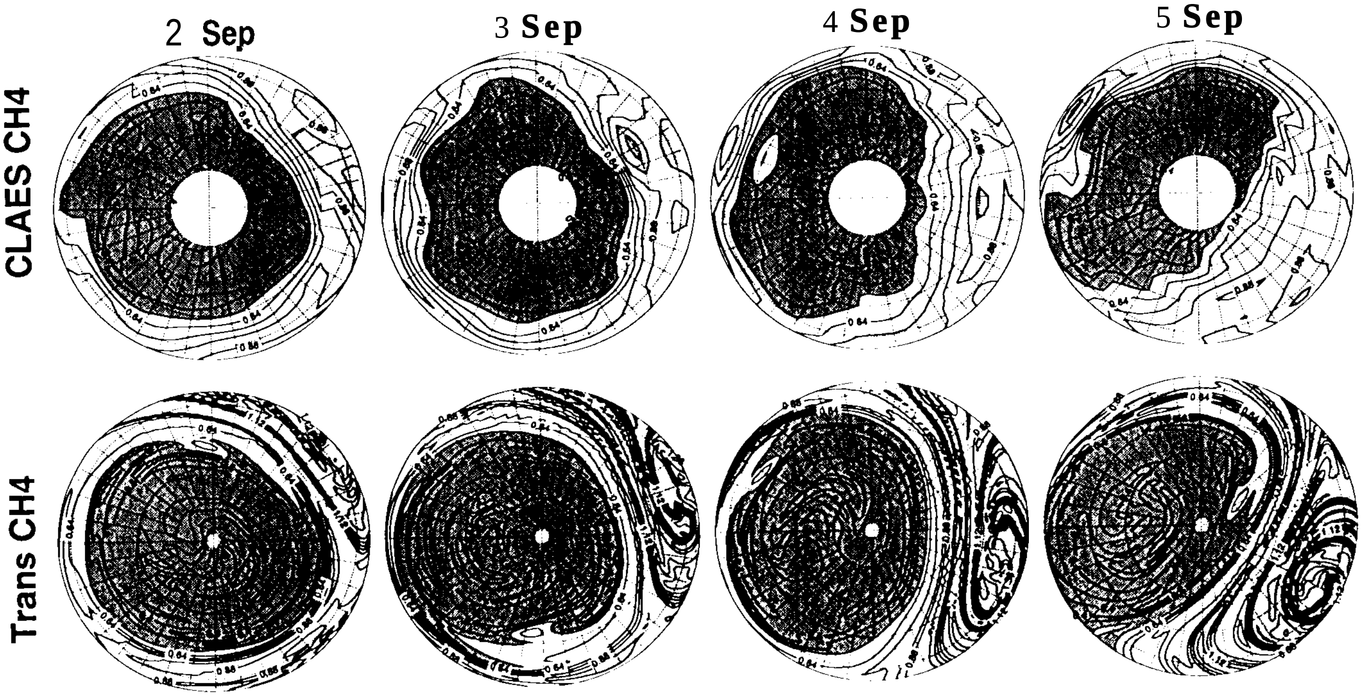

Fig. 13

UKMO scaled PV > 1.2 x le-4 1/s

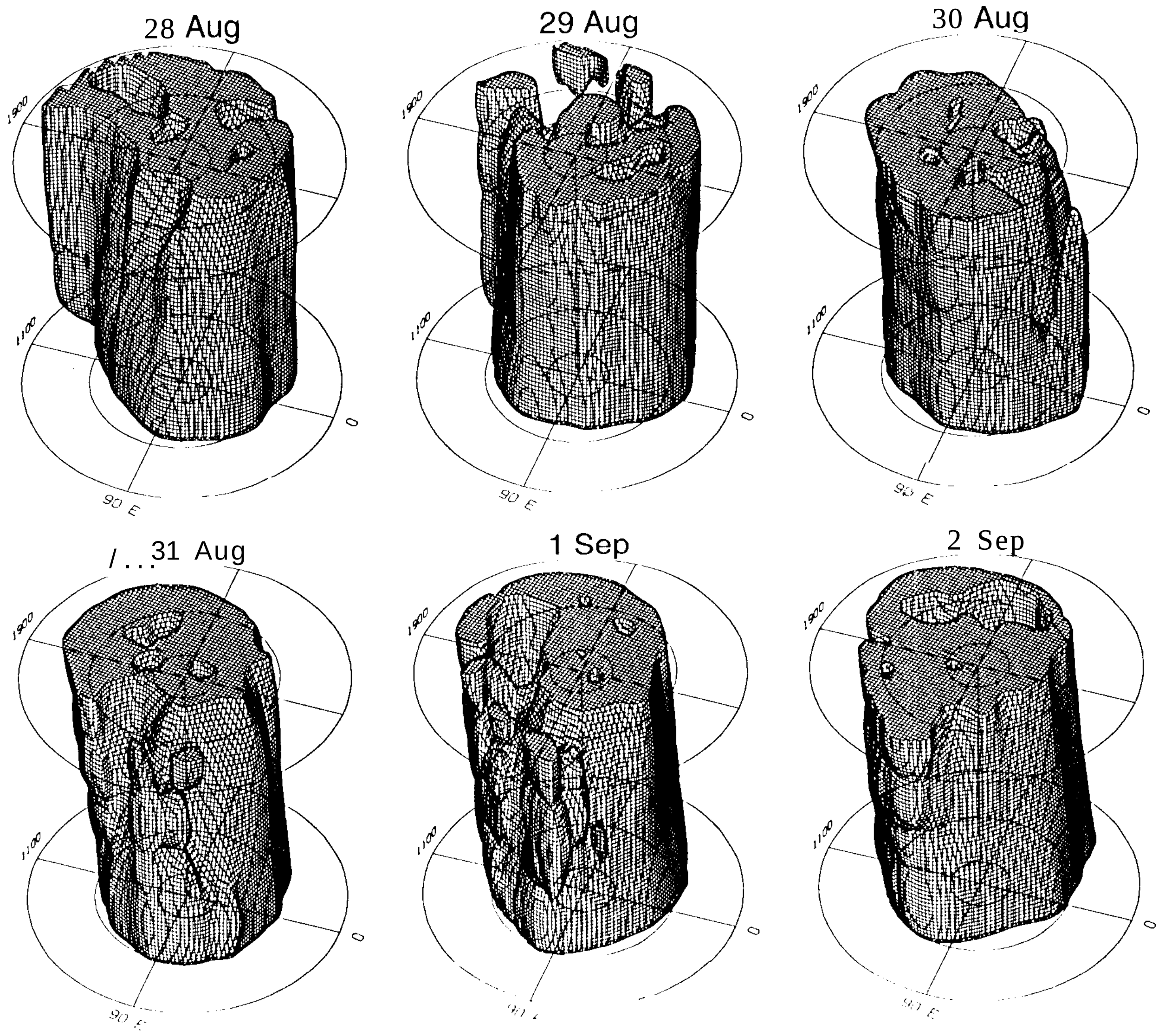

Fig. 15